NAVAL POSTGRADUATE SCHOOL

MONTEREY, CALIFORNIA

THESIS

ADAPTIVE CONTROL FOR FIXED WING AIRCRAFT

by

Ryan G. Beall

June 2017

Thesis Co-Advisors: Oleg Yakimenko
Vladimir Dobrokhdov
Second Reader: Fotis Papoulias

THIS PAGE INTENTIONALLY LEFT BLANK

Approved for public release. Distribution is unlimited

ADAPTIVE CONTROL FOR FIXED WING AIRCRAFT

Ryan G. Beall
LT, USN
B.S., United States Naval Academy, 2008

Submitted in partial fulfillment of the
requirements for the degree of

MASTER OF SCIENCE IN SYSTEMS ENGINEERING

from the

NAVAL POSTGRADUATE SCHOOL
June 2017

Approved by: Oleg Yakimenko
Thesis Co-Advisor

Vladimir Dobrokhdov
Thesis Co-Advisor

Fotis Papoulias
Second Reader

Ronald Giachetti
Chair, Department of Systems Engineering

THIS PAGE INTENTIONALLY LEFT BLANK

ABSTRACT

The field of adaptive control offers techniques for increasing performance and robustness in numerous settings and applications. Adaptive control is different than traditional feedback in that it offers a mechanism for adjusting the controller's parameters to reduce plant uncertainty. Traditional feedback control utilizes parameters, which are specified by the engineer to optimize an ideal use case, which often times requires extensive tuning and testing. Adaptive controllers adjust their control parameters using various intelligent mechanisms designed to increase robustness to plant variation or unanticipated disturbances. Adaptive control has many applications in the aerospace domain to include control strategies when aerodynamic coefficients are unknown or are non-constant, actuator failure, airframe damage, etc. This research evaluates fixed wing UAS controller performance and robustness using the $\mathcal{L}_1$ adaptive control architecture.

THIS PAGE INTENTIONALLY LEFT BLANK

Table of Contents

List of Figures

THIS PAGE INTENTIONALLY LEFT BLANK

List of Tables

THIS PAGE INTENTIONALLY LEFT BLANK

List of Acronyms and Abbreviations

DoD	Department of Defense
NPS	Naval Postgraduate School
USN	U.S. Navy
SISO	Single Input Single Output
CG	Center of Gravity
LTI	Linear Time Invariant
MAV	Mirco Aerial Vehcile
MEMS	Microelectromechanical Systems
MIMO	Multiple Input Multiple Output
MRAC	Model Reference Adaptive Control
NED	North East Down
PCHIP	Piecewise Cubic Hermite Interpolating Polynomial
PID	Proportional Integral Differential
UAS	unmanned aerial system
IMU	inertial measurement unit
ZOH	zero order hold

THIS PAGE INTENTIONALLY LEFT BLANK

Executive Summary

Executive Summary Here!.....

THIS PAGE INTENTIONALLY LEFT BLANK

Acknowledgments

I would like to thank.....

THIS PAGE INTENTIONALLY LEFT BLANK

CHAPTER 1:
Introduction and History

1.1 Problem Statement

The UAS has evolved tremendously over the past decade. Miniature autopilots have gotten smaller and cheaper with more sensitive and redundant sensor packages largely due to the cellular phone industry accelerating MEMs technology. The ability to manufacture these autonomous systems at fractions of the cost enables the advancement in multiple cooperative UAV applications including swarming capability. This ability to mass-produce large quantities of UAS's poses an interesting challenge. Even though the price has gone down and the performance has gone up, there still exists a significant amount of man-hours dedicated to sensor calibration and autopilot control law configuration and tuning for best achievable performance. Tuning from six to ten conventional PID controllers for a typical airframe is not an insignificant task. Imagine a swarming system that often use the same airframes potentially assembled by the same manufacturer and all aircraft still require a tedious quality assurance check. Physical aspects of the airframes such as CG, control surface deflection/calibration/speed, airframe alignment, etc. all can drastically vary within the same delivered batch of airframes. It should also be considered that most of these miniature UAS's experience hard landings, crashes, and/or damage in transportation, which all can effect aerodynamic handling qualities. In summary, conventional control laws require a moderate to high level of expertise at configuration stage and require significant man-hours to tune properly for every airframe even if identical.

UAS avionics have drastically improved over the past decade, but the fundamental control law algorithms have not changed. The PID architecture found it's origin in automatic ship steering applications in 1922 [**?**]. Conventional control law architectures for UAS's predominately still use PID controllers. Their architecture offers a well understood and predictable behavior and for this reason is well suited for the aviation application. The detriment of PID control is that it application is mostly constrained by the use on a linear plant and most aerospace applications are non-linear and time varying. An aircraft's control authority that increases proportionally to dynamic pressure is one example of aerodynamic

non-linear control behavior. In this case, the PID controller's robustness to changes in velocity and/or density altitude is not guaranteed and for most aircraft has to be delicately handled with lookup tables produced from hours of flight test.

1.2 Adaptive Control History

Adaptive control saw it's early debut in the NASA North American X-15 hypersonic rocket-powered X-plane experimental aircraft. The X-15's performance envelope exceeded mach 6.0 and 300,000 feet [**?**]. Engineers realized early on that the linear controllers performed well only at one dynamic pressure, but nowhere near the entire flight envelope. Scheduling the controller gains with respect to dynamic pressure (gain scheduling) was one method used to help ensure robustness; the method is still wide spread in commercial aviation due to its robustness but requires a lot of efforts to "explore" the entire flight envelop. This was when the initial benefits of adaptive control were becoming realized.

The X-15 program started in 1959 and continued to 1968 flying nearly 200 successful flights. It was considered one of NASA's most successful programs. The benefit of adaptive control to the X-15 was that the adaptive controller was supposed to adjust the gain parameters online automatically. If the controller was self tuning, it could potentially offer increased performance while reducing complexity. The Honeywell MH-96 adaptive controller was implemented in the X-15-3 as a fly-by-wire controller designed to adaptively adjust the damping in pitch and roll with respect to a desired model response. The goal was to achieve consistent aircraft response regardless of dynamic pressure and other variables. During test flights of the MH-96 adaptive control, increased performance was observed especially in the dynamic phases of reentry over that of the linear fixed gain damping system [**?**]. These early breakthroughs in adaptive control proved the benefits could be viable aerospace solutions. However, on November 15, 1967 there was a fatal accident caused by the adaptive controller. The adaptive controller created an out of control flight situation resulting in dynamic pressures exceeding the structural limits and subsequent breakup of the airframe at 65,000 feet.

The turbulent start of adaptive control as implemented on the X-15 program was largely due to the early naive understanding of robustness. Contemporary robust adaptive control strive to encapsulate these deficiencies of robustness in studies and proofs primarily using

Lyapunov stability analysis (FYI => Barbalat's lemma is used in stability proofs of negative semidefinite systems). In addition to the developments of rigorous stability tools, a number of unique techniques have also been implemented to further increase controller robustness although for the price of loosing some of its performance, see a detailed review of the most recent advances in []. One such technique utilizes dead band limits on the model adaptation process to avoid system/measurement noise from causing the un-learning of the states [**?**]. On the other hand, the $\mathcal{L}_1$ adaptive control algorithm utilizes a technique which seeks to decouple the adaptation rate from robustness by low pass filtering the adaptation estimator under the premise that estimating the entire frequency spectrum is overly ambitious and should be limited to the bandwidth of the actuator and plant. Many advances have been made in the adaptive control field over the past few decades and this research sets out to evaluate a small subset of these techniques in the unforgiving aerospace environment.

THIS PAGE INTENTIONALLY LEFT BLANK

CHAPTER 2:
Background and Literature Review

2.1 Preliminaries and Notation

This thesis uses the following notation, nomenclature, and fundamental equations of motion for fixed wing rigid body aerodynamics.

2.1.1 Kinematics

The following is the nomenclature that will be used to describe the kinematic equations. Euler angles for pitch (θ), roll (ϕ), and yaw (ψ) will have the units of radians. The following Figure 2.1 illustrates the North East Down (NED) reference frame definitions used for body rotational rates about the x axis (p), y axis (q), and the z axis (r) as well as the body velocities in the x axis (u), y axis (v), and the z axis (w).

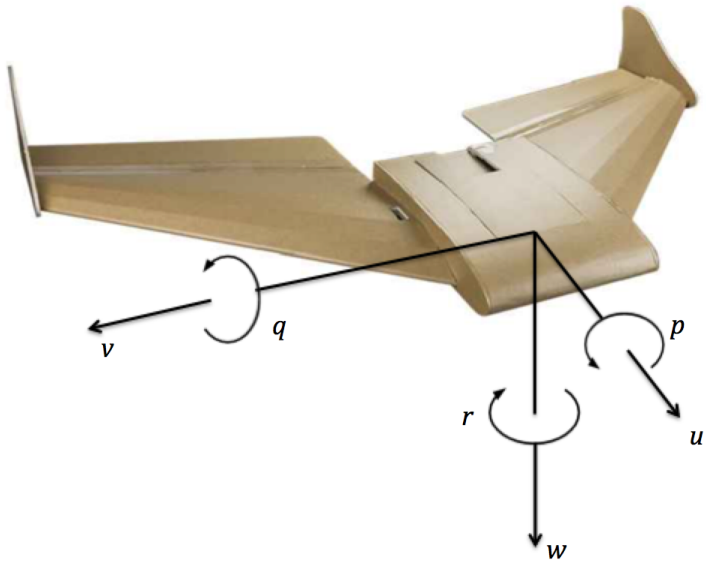

Figure 2.1. Reference frame - body rates and velocities

2.1.2 Transfer Functions

The modeling technique chosen for this research was the transfer function form. Transfer functions are used to describe the relationship between inputs and outputs of systems. This is accomplished using a series of polynomials. These polynomials are unknown for the aircraft and regression tools will be utilized to solve for them.

Transfer functions take the form:

$$H(s) = \frac{Y(s)}{X(s)} \tag{2.1}$$

where:

Y(s) is the Laplace transform of the output
X(s) is the Laplace transform of the input

Standard physics models of first and second order form are well understood and seen in many model derivations. The first order model takes the form:

$$H(s) = \frac{k_{dc}}{\tau s + 1} \tag{2.2}$$

where:

k_{dc} is the DC gain
τ is the system time constant (time in seconds to reach 63% of steady state)

Similarly the standard form for a second order system takes the form:

$$H(s) = \frac{\omega_0^2}{s^2 + 2\zeta\omega_0 s + \omega_0^2} \tag{2.3}$$

where:

ω_0 is the system natural frequency in radians per second
ζ is the system damping ratio

The modeling of a system can also be converted to a system of first order differential equations also known as state space modeling. The following nomenclature will be used to illustrate the modeling of first order systems where $\dot{x}$ is the time derivative of the state, A is the Hurwitz matrix, B is the input matrix, and u is the input vector.

$$\dot{x}(t) = Ax(t) + Bu(t) \tag{2.4}$$

2.2 Feedback vs Adaptive Control

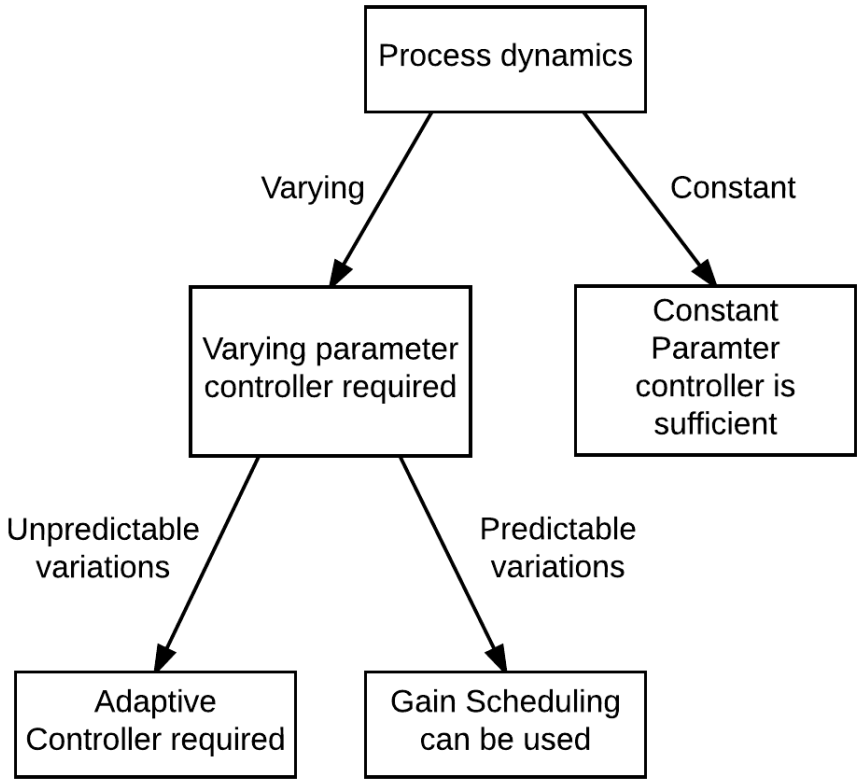

Figure 2.2. Determine if adaptive control should be used

2.3 Model Reference Adaptive Control

Model Reference Adaptive Control (MRAC) establishes the foundation for most of modern robust adaptive control. Its structure is intuitive in nature and seeks to define a system's response to a command signal with a reference model. Unlike traditional feedback where the error signal is generated with respect to state error, MRAC attempts to achieve a system response with respect to some reference model performance. MRAC assumes there there is some nominal response of the system which can be characterized with a model of unknown parameters. The error between the model response and the system response generates the error for an 'adjustment mechanism' to learn the unknown model parameters.

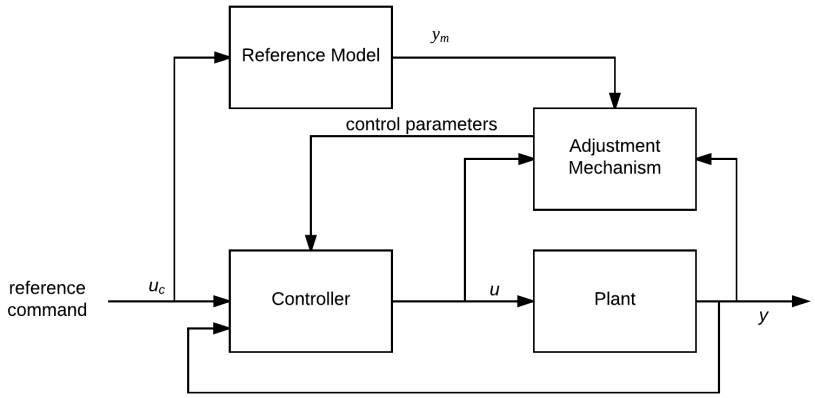

Figure 2.3. Traditional MRAC architecture

Figure 2.3 illustrates a topology where a traditional feedback controller is established as an inner loop and the 'Reference Model' and 'Adjustment Mechanism' is established as an outer loop. The outer loop attempts to minimize the error between the reference model output and the plant output. Using this error to learn the system parameters can be done utilizing one of two methods; gradient decent or stability theory.

2.3.1 MIT Rule - Gradient Decent

One of the first approaches to MRAC controllers was implemented at the Instrument Labs at MIT (now known as Draper Labs). The gradient decent based method was called the 'MIT Rule' for this reason [**?**]. This method attempts to learn some unknown parameter by descending the gradient of the error between the reference model and the plant output.

Given the simple first order system $G(s)$:

$$G(s) = k_{dc}\frac{1}{s+1} \tag{2.5}$$

where k_{dc} is some unknown feedforward gain. In the case of the MIT rule, k_{dc} is the parameter to be learned and is defined as θ. The first step in the MIT rule is to establish a cost (or loss) function. One example of a cost function $J(\theta)$ is:

$$J(\theta) = \frac{1}{2}e^2 \tag{2.6}$$

$$e = y - y_m \tag{2.7}$$

where e is error, y is the plant output, and y_m is the model output.

In order for the cost function to be minimized, the negative gradient of the cost function is calculated and used to correct the a priori estimate. This method takes the following form where γ is the adaptation gain:

$$\frac{d\theta}{dt} = -\gamma\frac{\partial J}{\partial \theta} = -\gamma e\frac{\partial e}{\partial \theta} \tag{2.8}$$

The stability of this method is very system dependent and heavily relies on trial and error to ensure the adaptation gain (γ) is not too high. This usually requires low adaptation rates for most systems and may not produce adequate results. It should also be noted that this method presupposes there is adequate persistence of excitation. Without a frequency rich error signal being generated by adequate persistence of excitation, the model will fail to adapt. This method also offers no guarantees that the learned parameters are actually the correct values.

2.3.2 Lyapunov Stability Criteria

Aerospace controllers tend to use linear controllers for their simplicity and well understood robustness characteristics. This is despite the fact that the applications of these linear controllers are applied to a non-linear dynamical system such as attitude control with varying dynamic pressure. Adaptive Controllers are non-linear and may offer performance

benefits to non-linear systems as seen in aforementioned aerospace applications. However, non-linear controller's robustness properties need to be evaluated. The Lyapunov stability criteria offers methods of evaluating these controller's boundedness and robustness behavior.

Aleksandr Lyapunov was a Russian mathematician who's work was published in 1892 [**?**] concerning the behavior of non-linear systems close to equilibrium without having to rigorously find the unique solutions to difficult differential equations used to model the system. His work was largely overlooked until the Cold War when aerospace solutions required a more rigorous approach to analyzing non-linear control robustness. Modern non-linear control engineers extensively utilize Lyapunov's techniques to design and evaluate non-linear controllers.

Lyapunov Stability Definitions

Lyapunov's methods attempt to evaluate autonomous nonlinear dynamical systems within the bounds of three classifications. In this case the autonomous system is defined as definable set of ordinary differential equations which are not explicitly dependent upon the independent variable. These classifications can be used to define a nonlinear system as Lyapunov stable, asymptotically stable, or exponentially stable.

Given the following autonomous nonlinear dynamical system:

$$\dot{x}(t) = f(x(t)), \qquad x(0) = x_0 \tag{2.9}$$

where f has equilibrium at x_e :

$$f(x_e) = 0 \tag{2.10}$$

then the equilibrium is said to be:

1. **Lyapunov Stable**
   for every $\epsilon > 0$ there exists a $\delta > 0$ such that, if $\left\|x(0) - x_e\right\| < \delta$, then for every $t \geq 0$ we have $\left\|x(t) - x_e\right\| < \epsilon$
2. **Asymptotically Stable**
   if the system is Lyapunov stable and there exists a $\delta > 0$ such that if $\left\|x(0) - x_e\right\| < \delta$,

then $\lim_{t\to\infty} \left\|x(t) - x_e\right\| = 0$

3. **Exponentially Stable**
   if the system is asymptotically stable and there exists $\alpha > 0, \beta > 0, \delta > 0$ such that if $\left\|x(0) - x_e\right\| < \delta$, then $\left\|x(t) - x_e\right\| \leq \alpha \left\|x(0) - x_e\right\| e^{-\beta t}$, for all $t \geq 0$

Being Lyapunov stable infers that if a system is near equilibrium then it will indefinitely remain near equilibrium. If the system if found to be asymptotically stable then it eventually will achieve equilibrium as $t \to \infty$ and being exponentially stable implies it reaches equilibrium even faster.

Lyapunov's Second Method

Lyapunov's second proposed method is also known as Lyapunov stability criteria. This method offers a less tenuous method for evaluating mathematically non-ideal systems. Lyapunov analysis of the linearized system around equilibrium can be cumbersome in the case where equilibrium is at the origin or the eigenvalues are purely imaginary. In this case, the solutions can rapidly depart to infinity or approach zero with little perturbation to the eigenvalues. Lyapunov's second method offers an alternative approach for classifying a systems stability using a concept that is similar to how energy is defined in classical dynamics.

Conceptually, Lyapunov's second method can be compared to evaluating the energy of a vibrating spring mass system. The energy of the unforced spring mass system will dissipate energy due to friction and or damping etc. This trend of energy leaving the system towards some 'attractor' is evidence of the system's stability characteristics and identifies that there will be some stable end state. Like wise, Lyapunov's second method characterizes this with the use of a Lyapunov candidate function $V(x)$. It is important to note that Lyapunov realized that the candidate function can be any function so as long as one candidate function is found in agreement with the stability criteria. It is then said to be Lyapunov stable if any candidate equation is found and meets the stability criteria. This means that it is only incumbent upon the engineer to find one candidate equation to meet the criteria. This can be an iterative process of trying multiple energy like equations. A common approach is to model the Lyapunov candidate equation as kinetic energy ($\frac{1}{2}u^2$). Lyapunov realized that characterizing the energy of a nonlinear system could be almost impossible for some cases, but this approach could prove stability without the rigorous knowledge of the true system's

energy.

Lyapunov's second method defines a system as Lyapunov Stable for a system $\dot{x} = f(x)$ having an equilibrium point at $x = 0$ where the Lyapunov candidate function $V(x) : \mathbb{R}^n \rightarrow \mathbb{R}$ such that:

- $V(x) = 0$ if and only if $x = 0$
- $V(x) > 0$ if and only if $x \neq 0$
- $\dot{V}(x) = \frac{d}{dt}V(x) = \sum_{i=1}^{n} \frac{\partial V}{\partial x_i} f_i(x) \leq 0$, for all values of $x \neq 0$

if $\dot{V}(x) < 0$ for $x \neq 0$ then system is asymptotically stable.

To determine if the system is globally stable, it is additionally required to prove the condition of radial unboundedness.

2.4 Other Adaptive Controllers

CHAPTER 3:
$\mathcal{L}_1$ Adaptive Control Derivation

Intro Here !!!!!!

Failures in early adaptive control were largely impart due to a very naive understanding of robustness. As paralleled in the X-15's robustness issues, Brian Anderson concludes that "it is clear that the identification time scale needs to be faster than the plant variation time scale, else identification cannot keep up" [**?**].

3.1 $\mathcal{L}_1$ Adaptive Control

The $\mathcal{L}_1$ adaptive controller is an evolution of the concepts implemented by MRAC. They are similar approaches designed to model a Linear Time Invariant (LTI) system with unknown constant parameters. These parameters are adjusted to achieve the desired outcome of the error between the actual plant (system) and the referenced system model (state predictor) to asymptotically approach zero. Adaptive control attempts to estimate the plant's unknown parameters in situ. Parameter estimation is done using either direct or indirect architectures. The indirect architecture attempts to estimate the system's parameters, which could be considered similar to system identification. Alternately the easier to implement direct architecture estimates the controller parameters explicitly. These architectures can be seen below in Figures 3.1 and 3.2.

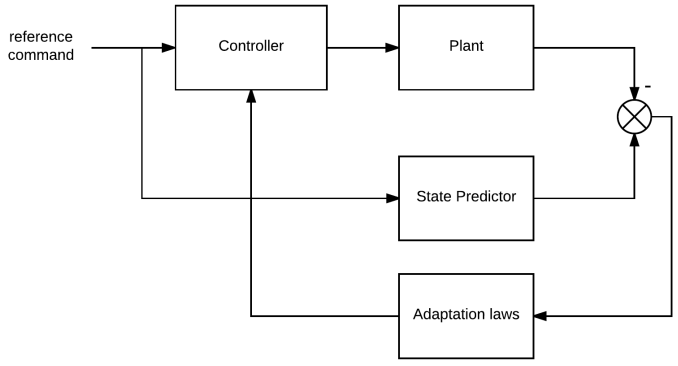

Figure 3.1. Direct MRAC architecture

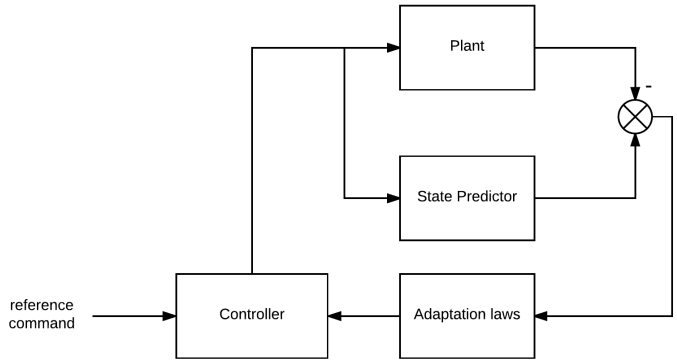

Figure 3.2. Indirect MRAC architecture

The $\mathcal{L}_1$ adaptive control algorithm asserts that trying to estimate the plant uncertainties outside of the control actuators' bandwidth is overly ambitious. The system's actuator bandwidth and the slow dynamics of the plant are most commonly the system's limiting factors, and the estimator's robustness/stability could be in question if un-modeled high frequency content exists in the plant. The $\mathcal{L}_1$ adaptive control constrains the objective function by using a low-pass filter (first or second order) to band the frequency response in order to meet robustness specifications. This low-pass filter should be tuned to a frequency response commensurate with the actuator's frequency response. When looking at examples of where to place the low-pass filter in the direct and indirect architectures, it becomes clear that the indirect architecture is the only candidate. Figures 3.3 and 3.4 illustrate the placement of the low-pass filter and its implication on the closed loop model.

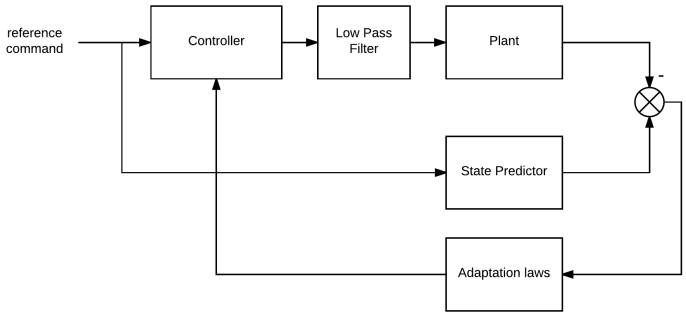

Figure 3.3. Direct MRAC architecture with low-pass filter

It can be seen that the low-pass filter in the direct architecture inherently changes the

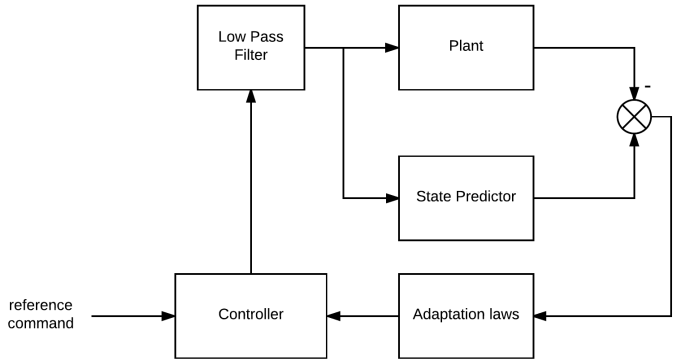

Figure 3.4. Indirect MRAC architecture with low-pass filter

structure of the model with the cascading of the low-pass filter and plant block diagrams. This change mathematically is not mirrored in the state predictor and therefore is not subtractable. However, in the indirect case, the structure of the model is kept intact and the low-pass filter is applied to both the plant and the state predictor. This ensures that the low-pass filter is subtractable when calculating the error state and the model's structure is kept intact.

In the primary literature for this research [**?**], the author often refers to the state predictor as the reference model or companion model for the direct and indirect architectures respectively. The reference model (direct architecture) intuitively maps the desired model response to the error feedback. In the indirect architecture case, the error state is a result of the companion model plus the low-pass filter. This subtle distinction is necessary because it must be accounted for when tuning the companion model with the included low-pass filter.

Many slight variations of the $\mathcal{L}_1$ adaptive architectures have been derived for various use cases [**?**]. Some of the following forms were studied for viability in the fixed wing unmanned aerial system (UAS) use case:

- Single Input Single Output (SISO) with constant but unknown state parameters
- SISO with time variant and/or nonlinear unknown state parameters
- Multiple Input Multiple Output (MIMO) with constant but unknown state parameters
- MIMO with time variant and/or nonlinear unknown state parameters

MIMO control algorithms would potentially afford the controller more ability to cope with

system coupling if present. A fixed wing UAS would exhibit coupled behavior due to the coupling present in the aerodynamics but was not chosen due to the added architectural complexity. Unknown state parameters that are assumed to be constant or time invariant are considered matched uncertainty. Unknown state parameters that are non-constant (time variant) and/or exhibit non-linear behavior are considered unmatched uncertainty. The unmatched uncertainty architecture offers a more appealing solution for fixed wing use cases (asymmetric actuator failure, aerodynamic coefficients scaled by dynamic pressure, etc.), but adds a significant amount of complexity to the architecture. In summary, the SISO architecture with matched uncertainty was chosen for this research.

The SISO controller with matched uncertainty was chosen to control pitch rate (q) and roll rate (p) of the aircraft using two separate but parallel controllers. This meant that the controller could be generalized to a first principles physical point mass model similar to derivations found in rigid body equations of motion. In this implementation of the $\mathcal{L}_1$ adaptive controller, the desired state x to be controlled was an individual body rate (e.g., q, p).

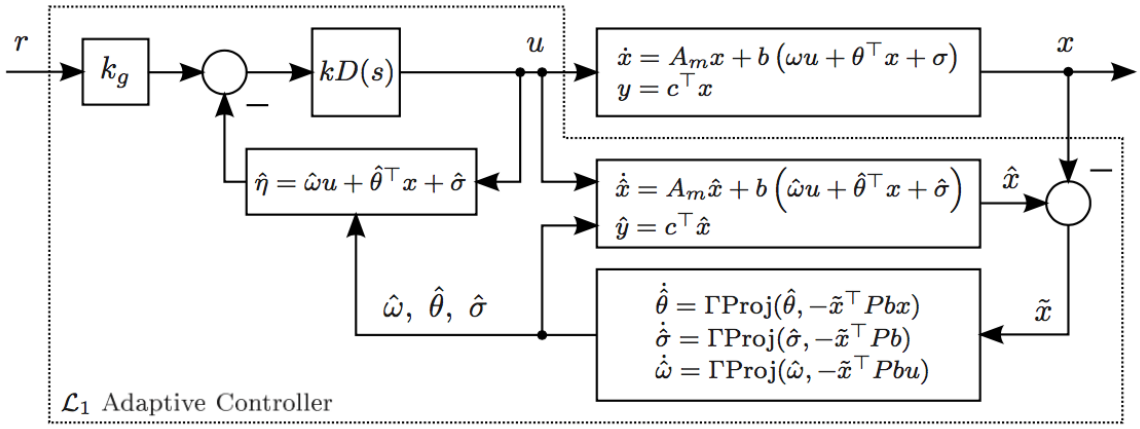

Figure 3.5. $\mathcal{L}_1$ Architecture with Matched Uncertainty Block Diagram [?]

As seen in Figure 3.5, the generalized $\mathcal{L}_1$ architecture in block diagram form and the following elements can be identified:

k_g - feed forward input gain
$kD(s)$ - user described filter (second order low pass plus integrator)
$\hat{\eta}$ - $\mathcal{L}_1$ controller state

$\dot{x}$ - first order differential equation of state model

$\hat{x}$ - state estimate

$\tilde{x}$ - state error

u - reference objective

A_m - Hurwitz matrix

b - input matrix

$\hat{\omega}$ - unknown input gain coefficient

$\hat{\theta}$ - unknown constant state coefficient

$\hat{\sigma}$ - unknown disturbance estimate

Γ - adaptation gain

Pb - solution to the Lyapunov stability criterion

It should also be noted that the architecture presented in Figure 3.5 includes the use of a projection operator. The parameters for $\dot{\hat{\omega}}$, $\dot{\hat{\theta}}$, and $\dot{\hat{\sigma}}$ are all projection based adaptation laws. This simply ensures that the adaptation stays bounded around the feasible region of parameter space. The Lyapunov stability proofs for this architecture rely on this method to guarantee stability [**?**] . More discussion on the specific application of this operator can be found in Appendix [???].

One of the main benefits of using the SISO architecture is that the solution to the Lyapunov stability criterion (Pb) used in the projection based adaptation laws is greatly simplified.

In this case, Pb reduces to:

$$Pb = \frac{1}{2\omega_n} \tag{3.1}$$

where ω_n is the natural frequency in rad/s for the companion model in discrete recursive form assuming DC gain of 1.

3.2 $\mathcal{L}_1$ Discrete Time Implementation

THIS PAGE INTENTIONALLY LEFT BLANK

CHAPTER 4:
Design of Experimental Platform

4.1 Autopilot

4.2 Simulation

4.3 Airframe

The aircraft used for this research was the Flitetest Spear [**?**]. The Spear airframe was chosen for its endurance capability of greater than 45 minutes of flight time and it's large capacity fuselage. The flying-wing architecture keeps the actuation requirement to a minimum of two servos by utilizing an elevon configuration.

Figure 4.1. Spear Airframe

The large blunt nose provides adequate space for two 2,200 mAh (12.6volts) lithium polymer batteries wired in parallel. The remaining cargo space was used for accommodating the Pixhawk autopilot.

This plane was constructed out of craft foam board. The plans were downloaded from flitetest.com [**?**] and converted to CorelDraw vector files for use in a laser cutter. These files were then cut out of four sheets of foam board using the laser cutter. The wing halves were joined with standard box tape and hot-glue. This provided a cheap and rapid construction process which was achievable under four hours of build time.

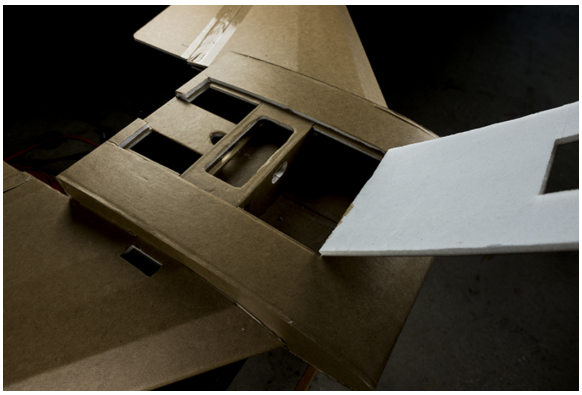

Figure 4.2. Spear Cargo Capacity

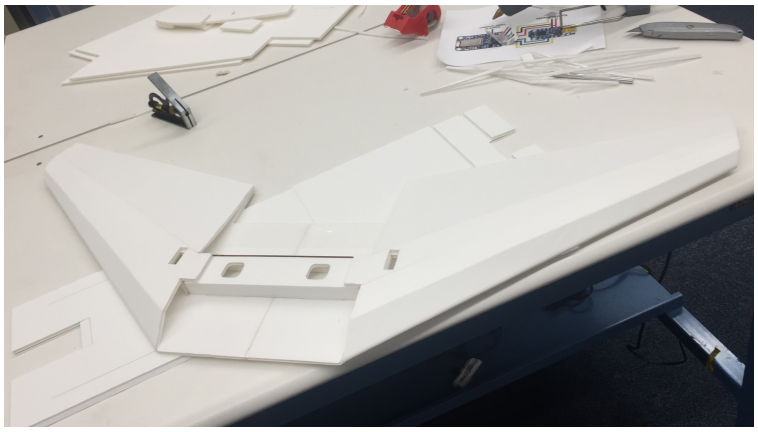

Figure 4.3. Spear Build Process

The aircraft specifications are as follows:

- Weight without battery: 1.45 lbs (658 g)
- Center of gravity: 3 – 3.5” (76 – 89 mm) in front of firewall
- Control surface throws: 16°deflection – Expo 30%
- Wingspan: 41 inches (1041 mm)
- Recommended motor: 425 sized 1200 kv minimum
- Recommended prop: 9 x 4.5 CW (reverse) prop
- Recommended ESC: 30 amp minimum
- Recommended Battery: (2) 2200 mAH 12.6 volt minimum
- Recommended Servos: (2) 9 gram servos

CHAPTER 5:
Flight Testing and Performance Evaluation

5.1 Simulation Results

5.2 Flight Test Results

5.2.1 Data Collection

The Pixhawk autopilot was used to capture roll and pitch rates $(\dot{p}, \dot{q})$ for the test vehicle as well as the pilot's command inputs. These outputs and inputs were the essential building blocks for creating pitch rate and roll rate models for the test vehicle. The autopilot is capable of logging data at 50-200 Hz and therefore is a discrete time domain signal. This data should ultimately be manipulated into the s-domain. The mathematics for this procedure are well defined and numerous tools can be used to simplify this process.

It is crucial to ensure there is sufficient frequency content in the data recorded. Exciting multiple frequencies in the time domain ensures the regression techniques have an adequate sample space to search for polynomial coefficients. Exciting adequate frequency inputs is analogous to only sampling at one independent variable and expecting to get a regression fit from a non-changing dependent variable.

To ensure sufficient frequency content was obtained from the aircraft, a linear chirp was chosen and implemented into the Pixhawk source code as follows:

$$x(t) = sin\left[\phi_0 + 2\pi\left(f_0 t + \frac{k}{2}t^2\right)\right] \tag{5.1}$$

where:

ϕ_0 is the initial phase of the chirp at t=0 (nominally zero degrees)
f_0 is the initial frequency at t=0
k is the chirp rate

t is time in seconds

An example of this formulation can be seen below:

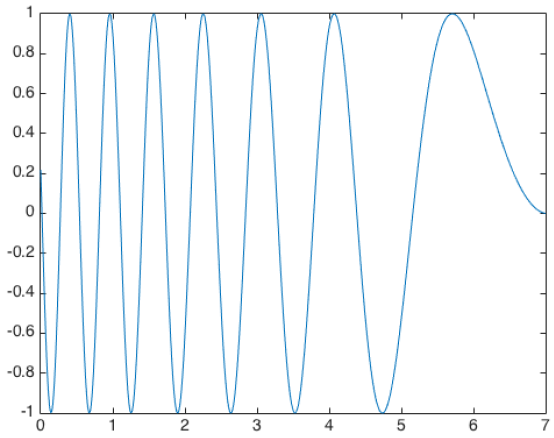

Figure 5.1. Reverse Linear Chirp Example

5.2.2 Model Regression

With the logged input and output data in discrete form, the data needs to be further shaped to properly convert to an s-domain representation. The first step is ensuring that the data is of constant sampling rate. In other words, the time between samples is uniform from sample to sample. The data provided from the Pixhawk autopilot does not have a uniform sampling rate. The sample rate is a user-defined rate (50-200Hz), but has a slight amount of jitter (±0.1%). Piecewise Cubic Hermite Interpolating Polynomial (PCHIP) interpolation was used to interpolate the data into a uniform sampling rate.

After the data is shaped correctly with a uniform sample rate, the discrete data is transformed into a continuous approximation using a zero order hold (ZOH) technique. Taking the Laplace transform of the continuous input/output data will convert it into the s-domain and finally a non-linear least squares minimization algorithm can be run to find the polynomial coefficients which best fit the data.

The order of the regression (number of polynomials to estimate) is at the discretion of the engineer and their intuition of system's physical representation. Higher order models will better fit the data, but in most cases tend to over fit the data if they cannot be justified by physical principles. Most aircraft models assume that the system is LTI and second order.

These fundamental aerodynamics models divide the modeling into longitudinal and lateral dynamics. Essentially each axis of the aircraft is assigned two second order responses. Pitch, for example, has a second order response in the pitch damping mode (also known as the short period) and also has a second order response in the transition of kinetic energy to potential energy (also known as the long period or phugoid). This would imply that the collected body rate data $(\dot{p}, \dot{q})$ collected by the autopilot should be modeled as first order systems because body rate is the first derivative of attitude. Assuming a first order system for the collected data in this experiment keeps the originally derived physical meaning but may be insufficient upon critical analysis. Both first order and second order model were estimated for comparison sake.

Results were collected from two flight test events. The first flight test was data collected prior to implementing the chirp and the pilot attempted to increase frequency of the input signal manually. The second set of data collected was via the reverse linear chirp method previously described.

The manually piloted acquired data was expected to not have as adequate of frequency content in the signal but still provided adequate results for modeling the aircraft.

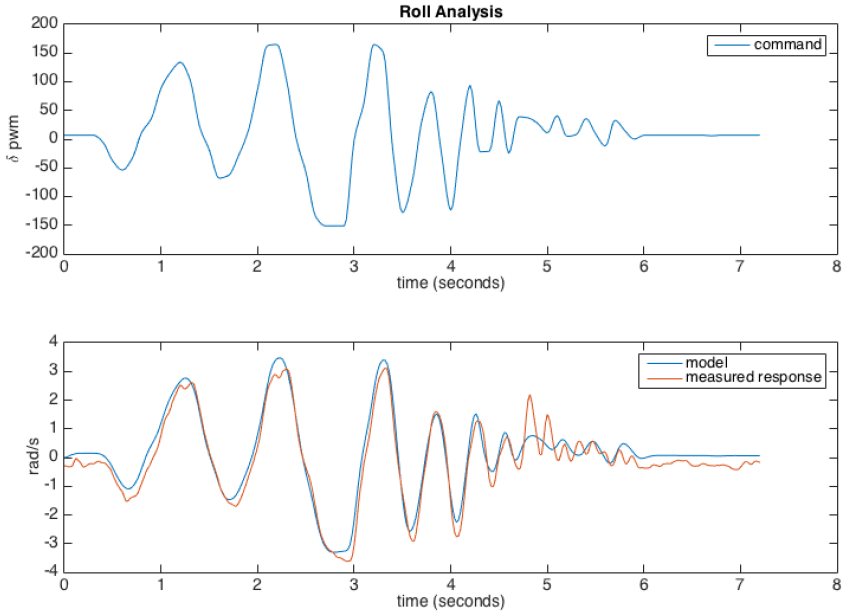

Figure 5.2. Roll Model Regression with Manual Inputs

The above result demonstrates the utility of this technique even with poorly structured data

from manual pilot inputs. It can be seen that the second order model starts to misrepresent the data at higher frequencies. The lower frequency validity of this model showed potential and most of the high frequency response may able to be neglected upon further review. The following figure with the chirp results highlights the actual issue with the high-frequency modeling issues.

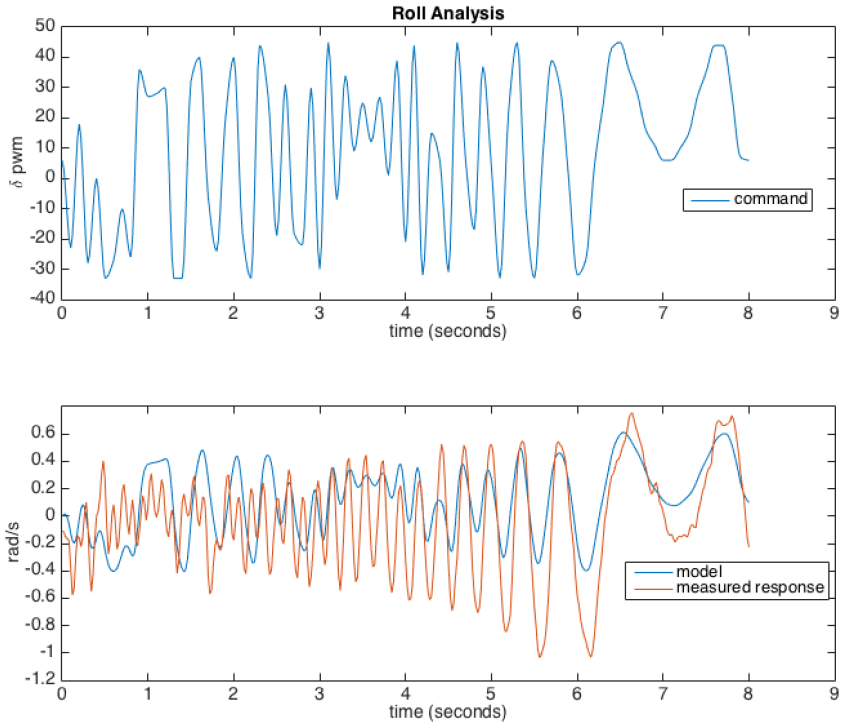

Figure 5.3. Roll Model Regression with Reverse Linear Chirp

The reverse linear chirp, starting at high frequency and chirping down, clearly illustrates that this regression method has an underlying problem that was not evidently clear in the previous example. In the chirp analysis, it is clear that the high frequency modeling is in error. After reviewing this result, it was clear that the sampling rate of the input channel was aliased. The chirp response was physically observed on pre-flight, in actual flight, and in the actual body rate of the aircraft. However, the aliased input channel was arbitrarily biasing the regression result. The data was logged at 50 Hz with the assumption that 50 Hz was 10 times higher than the expected natural frequency of the aircraft and at least five times higher than the Nyquist criterion. The Nyquist criterion is the theoretical minimum frequency ($2f_0$) to sample a signal and recover a given frequency. This result clearly illustrates that 50

Hz data sampling rate was not high enough to properly capture the input channel without biasing. The recommendation going forward is to increase the sampling rate to as high as reasonably achievable (200Hz).

The manually piloted acquired data was selected as the most viable data source for the models. There were two separate tests run on the same aircraft on the same flight and the following is the results using this regression technique to model a second order system.

$$H(s) = \frac{10.39}{s^2 + 31.26s + 504.9} \tag{5.2}$$

and

$$H(s) = \frac{10.61}{s^2 + 29.77s + 498.7} \tag{5.3}$$

Converting to standard form as described in equation 2.3:

$$H(s) = \frac{0.0206 * 22.47^2}{s^2 + 2 * 0.69s + 22.47^2} \tag{5.4}$$

and

$$H(s) = \frac{0.0213 * 22.33^2}{s^2 + 2 * 0.67s + 22.33^2} \tag{5.5}$$

It is important to note that this system identification technique run on separate sets of data has produced two models with very similar values for ω_n and ζ.

This produces the average values of:

$\omega_n = 22.4 rad/s$
$k = 0.0209$
$\zeta = 0.681$

In the author's experience, these values are reasonable values for this size and weight of airframe. This regression technique has shown potential to create realistic models from actual flight test data. The data must be properly shaped and improved models would result if the data logging rate was increased. The chirp method has the potential to increase the fidelity of the high frequency response of the aircraft if the aliasing issue can be resolved on the command input channel.

CHAPTER 6:
Recommendation

THIS PAGE INTENTIONALLY LEFT BLANK

CHAPTER 7:
Conclusion

THIS PAGE INTENTIONALLY LEFT BLANK

Initial Distribution List

1. Defense Technical Information Center
   Ft. Belvoir, Virginia

2. Dudley Knox Library
   Naval Postgraduate School
   Monterey, California